Numerical calculation of supercritical Dirac resonance parameters by analytic continuation methods

Edward Ackad and Marko Horbatsch
Department of Physics and Astronomy, York University, 4700 Keele Street, Toronto, Ontario, Canada M3J 1P3
(Received 11 November 2006; published 21 February 2007)

The spectrum of the Dirac equation for hydrogenlike systems with extended nuclei becomes complicated when the nuclear charge exceeds a critical value $Z \approx 170$, since the lowest bound state becomes a resonance in the negative energy continuum. We address the problem of computing the resonance parameters by extending the mapped Fourier grid method to incorporate either complex scaling of the radial coordinate, or alternatively a complex absorbing potential. The method is tested on the case of quasimolecular collisions in the monopole approximation.

DOI: 10.1103/PhysRevA.75.022508 PACS number(s): 31.30.Jv, 31.15.−p, 14.60.Cd, 12.20.−m

I. INTRODUCTION

The spectrum of hydrogenlike atoms represents a textbook example both in nonrelativistic and in relativistic quantum mechanics. In the relativistic case of the Dirac-Coulomb problem with pointlike nuclei problems arise for $Z\alpha \geq 1$ [1]. Recently it was shown that solutions are possible for any value of the nuclear charge Z, when self-adjoint extensions of the Hamiltonian are introduced [2]. For large Z, the effects of extended nuclei become important [3,4]. For very large values of $Z \gtrsim 170$ the $1S_{1/2}$ energy eigenvalue merges with the negative continuum ($E \lesssim -mc^2$). The interpretation worked out by the Frankfurt group is that the $1S_{1/2}$ state becomes a resonance for $Z > Z_{cr}$ [5]. The precise value of Z_{cr} depends on the model for the extended nucleus [3].

Given that no ordinary nuclei exist with charges in this range one might consider the problem an academic one. However, in the context of heavy-ion collisions near the Coulomb barrier an adiabatic treatment of the inner electron shells is called for (due to the slow-down of the nuclear motion caused by the Coulomb repulsion) [5–8]. Therefore, the problem resurfaces in the context of the monopole approximation to the full time-dependent two-center problem. When a K-shell vacancy is brought into the collision it couples resonantly to the filled negative-energy continuum once the system becomes supercritical. This coupling then leads to a breakdown of the perturbative QED vacuum [1].

Systematic studies of resonance parameters in atomic physics are usually performed by so-called dilation methods where the radial position coordinate is rotated into the complex plane. Recent advances in such techniques in nonrelativistic quantum mechanics can be found in the literature [9,10]. The goal is to modify the resonance wave function so that it becomes square integrable. The eigenvalue problem becomes non-Hermitian and the resonance parameters are given by a complex energy eigenvalue. Details on how to deal with the non-Hermitian eigenvalue problem have been given recently [11]. The method of complex rotation (scaling) has been used, e.g., to compute Stark-level parameters [12,13], and electron-atom [14] and electron-molecule resonance states [15]. For the relativistic Dirac case, the Stark resonance parameters have been computed only recently by this technique in the weak relativistic limit [16]. Complex scaling has also been used in the context of relativistic many-body perturbation theory [17].

In the present work, we apply two analytic continuation methods to the problem of supercritical $1S_{1/2}$ Dirac resonances, namely the complex scaling (CS) method and the method of a complex absorbing potential (CAP). The technique to construct a matrix representation of the Dirac Hamiltonian is an adaptation of the mapped Fourier grid method [18,19] which we applied recently to the ordinary Dirac-Coulomb problem [20].

The diagonalization of a matrix representation of the Hamiltonian provides a discretized spectrum with positive-energy and negative-energy quasicontinuum states which span a large range of energies. We demonstrate that a direct application of the Hermitian method yields a representation of the supercritical resonance as a superposition of these continuum states. Once we apply one of the analytic continuation techniques the supercritical resonance is represented by a single state. This allows for a more accurate determination of the resonance parameters.

II. THEORY

A. Supercritical resonances

In single-particle quantum mechanics bound states become resonances when the potential is modified such that the previously bound particle can escape to infinity (e.g., when the linear Stark potential is added to the Coulomb interaction). More generally for a system which has sufficient energy to break up into two or more subsystems a scattering state is called resonant if it is long-lived compared to the collision time [21,22]. Such a state is described by the mean energy position E_{res} (which is usually shifted from the bound-state eigenenergy), and by the lifetime τ. The latter provides a measure of the decay time of an initially prepared quasibound state. In scattering theory, the total cross section resonates if the particle energy is close to E_{res} and can be described by a Breit-Wigner shape, which is characterized by a width parameter Γ. According to the uncertainty principle the temporal behavior of a decaying bound state and the cross section shape are related by $\Gamma\tau \sim \hbar$. A determination of Γ normally requires a solution of the scattering problem for

many energies in the vicinity of E_{res} and a fit of the phase shifts to the Breit-Wigner shape.

In analytic continuation methods the resonance parameters E_{res} and Γ are determined from a non-Hermitian eigenvalue problem with eigenenergy $E_R = E_{\mathrm{res}} - i\Gamma/2$. Without complex scaling, the eigenstates (called Siegert states) are non-normalizable (exponentially divergent). The dilation transformation makes them square normalizable and amenable to calculation by basis-state expansion. An alternative to the dilation transformation is the addition of a complex absorbing potential at large distances.

Supercritical resonance states occur when the attractive Coulomb potential, modified at short distances to account for a finite nucleus, becomes deep enough such that the energies of some low-lying bound states fall below $-mc^2$. These negative-energy resonances are qualitatively similar to resonances embedded in a positive-energy continuum and can be characterized by discrete complex energies. In contrast to resonances embedded in the positive continuum, supercritical resonance energies are given by $E_R = E_{\mathrm{res}} + i\Gamma/2$. This is understood by reinterpreting the supercritical resonance for an electron with negative energy as a positive-energy positron resonance propagating backwards in time according to CPT symmetry. The time reversal transformation necessitates a positive imaginary part of the energy eigenvalue to ensure that the state decays as time propagates to negative infinity. In order to calculate the supercritical resonance parameters the Hamiltonian is analytically continued (either by complex scaling or by adding an imaginary long-range potential) in order to break the hermiticity of the Hamiltonian, which results in complex eigenvalues [21].

B. Complex scaling

Complex scaling introduces an analytic continuation of the Hamiltonian by a transformation of the reaction coordinate by $r \to re^{i\theta}$, where θ is a real parameter (rotation angle). It has been used extensively in atomic and molecular physics and has been put on firm mathematical grounds by Reinhardt [22] and Moiseyev [21]. Recently it was applied to the case of Stark resonances in the Dirac equation [16]. Increasing θ in small steps from zero results in a series of energy spectra where the continuum-state energies are increasingly rotated into the complex energy plane with the branch cuts as pivot points. The bound states remain on the real axis and are not affected by the change in θ. As θ is increased from zero the resonance states initially rotate with the neighboring continuum states, but then stabilize at the resonance energy, and remain relatively stable for a range of θ values (this is why the method is also referred to as the stabilization method). The closest approximation to the resonance energy occurs at the most stable energy eigenvalue along the θ trajectory, which is found where $\left(\left|\frac{dE_R}{d\theta}\right|\right)$ is minimized.

C. Complex absorbing potential

Adding a complex absorbing potential to the Hamiltonian is an alternate way of analytically continuing the Hamiltonian, and has been put on firm mathematical grounds by Riss and Meyer [23]. An illustration of why the method works was given recently by Santra [24]. Several authors have used this method with the Schrödinger equation [25–31], yet no work in the literature is known to us where the CAP has been used with the Dirac equation. To augment the Dirac Hamiltonian, the CAP should transform as a scalar,

$$\hat{H}_{\mathrm{CAP}} = \hat{H} - i\eta\hat{\beta}\hat{W}(r), \tag{1}$$

where η is a non-negative parameter determining the strength of the CAP, $\hat{\beta}$ is the standard Dirac matrix [1], and $\hat{W}(r)$ is a function tailored for the specific problem. Its properties are chosen such that the "bound" part of the resonance state is not deformed significantly, i.e., one chooses a potential function which is nonzero in the asymptotic region only. The procedure for revealing the resonances is similar to that of CS. The strength of the CAP is increased from $\eta=0$ in small steps which yields a sequence of eigenvalue spectra as a function of η. To identify the resonance energy one searches for the minimum of $\left(\left|\eta\frac{dE_R}{d\eta}\right|\right)$ along the η trajectory [23].

D. Matrix representation from the mapped Fourier grid method

Both the CS and CAP methods are usually implemented in a matrix representation. Of particular importance to resonance problems is the coupling to continuum states. The mapped Fourier grid method provides an efficient representation of the Hamiltonian and yields a systematic discretization of its continuum spectrum [20]. It works by first mapping the semi-infinite radial coordinate to a finite equidistant parameter $\phi \in [0, \pi]$. The mapping function is chosen to allocate many points near the origin and then at increasingly sparse intervals further from the origin. We choose

$$r(\phi) = [s\phi - 4000\arctan(s\phi/4000)]/(\phi - \pi)^2. \tag{2}$$

The parameter s of the mapping function allows for a tailoring of the grid to a given potential. The solution to the Dirac equation is then expanded into a finite sine series given by

$$f(r(\phi_i)) = \sum_{m=1}^{N} b_m \sin(m\phi_i), \tag{3}$$

$$\frac{df(r(\phi_i))}{d\phi} = \sum_{m=1}^{N} m b_m \cos(m\phi_i), \tag{4}$$

where without approximation

$$b_m = \frac{2}{N+1}\sum_{n=1}^{N} f(r(\phi_n))\sin(m\phi_n). \tag{5}$$

The set $\{\phi_i : i = 1, \ldots, N\}$ defines the radial collocation points.

Upon diagonalization of the matrix representation of size $2N \times 2N$, one obtains N negative energy states, and a total of N bound and positive continuum states. For supercritical Hamiltonians, an increased density of states occurs in the vicinity of the supercritical resonance energy. This is demonstrated in the next section.

III. RESULTS

While it is possible to solve the Dirac equation for a single extended nucleus of supercritical charge $Z>170$, no evidence exists for such exotic elements. Therefore, we use a physically relevant model of two extended nuclei separated by distances of the order of a few nuclear radii. In this work we focus almost exclusively on the $U^{92+}+Cf^{98+}$ system at a distance of $R=20$ fm in the monopole approximation. We compare results from the two analytic continuation methods to previous literature values. At the separation of $R=20$ fm the ground state, $1S\sigma$ is embedded into the negative-energy continuum as a supercritical resonance at about $-1.76mc^2$, i.e., well below the negative continuum boundary. The nuclear radius is taken to be $R_n=1.2\sqrt[3]{A}$ fm, where A is the number of nucleons (in our case $A_U=238$ and $A_{Cf}=251$). The nuclei are assumed to be displaced homogeneously charged spheres with a separation of R between the charge centers. In the center-of-mass frame the monopole potential for each of the two nuclei with respective charge Z_i, radius $R_n^{(i)}$, and center-of-mass displacement $R_{\text{c.m.}}$is given (in units of $\hbar=c=m_e=1, Z=Z_i, R_n=R_n^{(i)}$) by

$$V(r)=\begin{cases} -\dfrac{Z\alpha}{r} & \text{for } r>r_+, \\ -\dfrac{Z\alpha}{R_n^3 R_{\text{c.m.}}}\left(\dfrac{(R_{\text{c.m.}}-R_n)^3(R_{\text{c.m.}}+3R_n)}{16r}-\dfrac{r_+^2(R_{\text{c.m.}}-2R_n)}{4}+\dfrac{3(R_{\text{c.m.}}^2-R_n^2)r}{8}-\dfrac{R_{\text{c.m.}}r^2}{8}+\dfrac{r^3}{16}\right) & \text{for } r_-<r<r_+, \\ -\dfrac{Z\alpha}{R_{\text{c.m.}}} & \text{for } r<r_-, \end{cases} \tag{6}$$

where $r_\pm=R_{\text{c.m.}}\pm R_n$ [32]. The expression is obtained from the potential for a homogeneously charged sphere displaced by $R_{\text{c.m.}}$ along the z axis and then expanded in Legendre polynomials.

The mapped Fourier grid method can provide approximate resonance parameters directly without analytic continuation methods. Even though it is unlikely that a discretized continuum eigenstate of the Hamiltonian matrix will fall exactly on the mean energy of the resonance, the closer such a state is to the mean energy the more it resembles the resonance state. The bound (small-distance) part of a supercritical $1S\sigma$ resonant state is similar to a subcritical $1S\sigma$ state. The inner product of a normalized subcritical and supercritical $1S\sigma$ equals approximately one, and thus the projection of a subcritical $1S\sigma$ onto the supercritical basis states shows how similar the latter states are to a bound state.

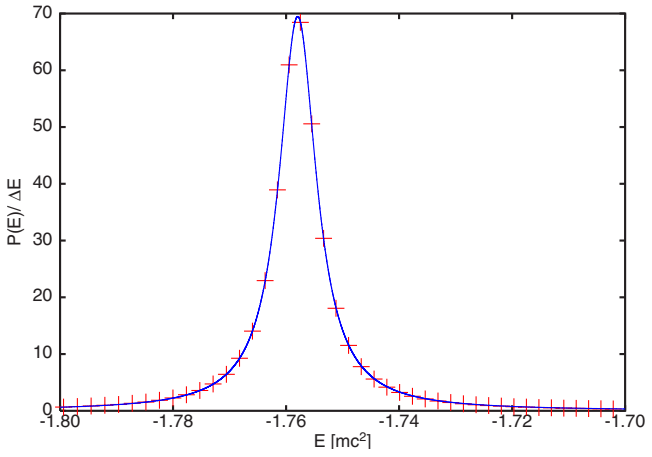

FIG. 1. (Color online) The projections $|\langle\phi(E_\nu)|\psi_{1S\sigma}\rangle|^2/(E_\nu-E_{\nu-1})$ of a bound $\psi_{1S\sigma}$ state onto the supercritical U-Cf quasicontinuum states $\phi(E_\nu)$ (calculated for a $N=3900$ and $s=6000$ basis) are shown as crosses (+). The subcritical bound $\psi_{1S\sigma}$ was obtained for a separation of $R=45$ fm, while the supercritical basis is for $R=20$ fm. The line represents a Breit-Wigner fit to the data with $E_{\text{res}}=-1.757\,95mc^2$ and $\Gamma=4.12$ keV for the U-Cf system at $R=20$ fm.

A plot of the square modulus of this inner product, P, displays the resonance shape as shown in Fig. 1. By fitting the data to a Breit-Wigner distribution the parameters of the supercritical resonance (E_{res},Γ) are obtained without the need to subtract a background. This provides a direct and independent verification of the analytic continuation methods discussed below. The result is, however, sensitive to the particular subcritical $1S\sigma$ used for the calculation of P.

The resonance parameters can also be calculated by fitting the Breit-Wigner shape to the density of states as shown in Fig. 2. We obtain the density of states (in arbitrary units) by calculating

$$\rho\left(\frac{E_{\nu+1}+E_\nu}{2}\right)=\frac{1}{E_{\nu+1}-E_\nu}, \tag{7}$$

where E_ν are the quasicontinuum eigenvalues. The fit requires the approximation to the local background density, and, thus, the results are somewhat sensitive to the form of the fit. Using a single rational term for the background with a Breit-Wigner distribution added the density of states is fitted in Fig. 2 by

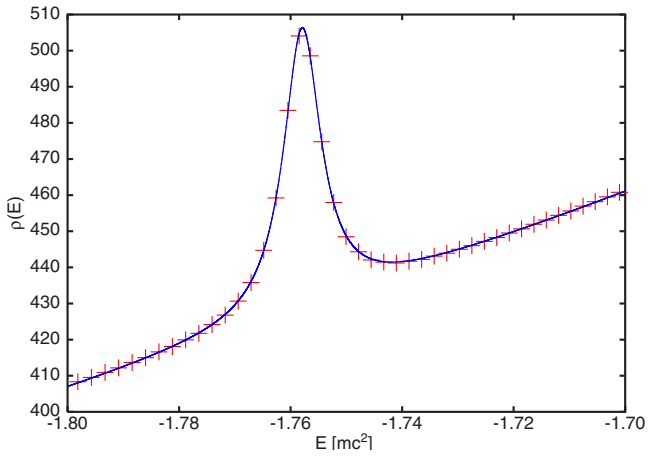

FIG. 2. (Color online) The density of states Eq. (7) from a Hermitian matrix diagonalization for the U-Cf ($R=20$ fm) Hamiltonian obtained with a basis with $N=3900$ states and $s=6000$, is shown by crosses (+). The line shows a fit with Eq. (8), and yields $E_{\rm res}=-1.757\,94mc^2$ and $\Gamma=4.17$ keV.

$$\rho(E_\nu) = \frac{A_1}{|E_\nu|^q} + A_2 \frac{\Gamma/2}{(E_{\rm res}-E_\nu)^2+\Gamma^2/4}, \tag{8}$$

where A_1, A_2, and q are fit constants. For both methods some inaccuracy is introduced by the choice of energy window to which the fitting procedure is applied. The analytic continuation methods discussed below are free from these problems.

Figures 1 and 2 also provide an indication of the energy resolution achieved by the present implementation of the mapped Fourier grid method. In a matrix representation obtained by conventional localized basis sets it would be difficult to attain this level of resolution. Nevertheless, we call the present discretization a quasicontinuum, since it is clear that each discretized continuum state has a finite energy width associated with it, i.e., it really does represent a wave packet state.

For the present problem there is no barrier in the potential. However, as explained by Reinhardt *et al.* [5] one can find the region where the supercritical resonance state displays tunneling behavior by looking at the intersection of $E_{\rm res}$ with the curve $V(r)-mc^2$. For our case this occurs at $r_V \approx 2$ (in units of $\hbar/m_e c$).

For the calculations with complex absorbing potential we choose the polynomial form

$$W(r) = \Theta(r-r_c)r^n, \tag{9}$$

where Θ is the Heaviside step function and $n \geq 1$. When using a linear absorber ($n=1$) we found that the resonance parameters $(E_{\rm res},\Gamma)$ do depend on the choice of r_c, but are least sensitive when $r_c \simeq r_V$. In fact, we observe a minimum for the width parameter, Γ, at $r_c=r_V$ as seen in Fig. 3. For a quadratic CAP ($n=2$) there is minimal variation in the extracted resonance parameters on the same scale.

We can draw a few conclusions from these results. The linear CAP through the sensitivity of the result to the value of r_c, is providing support to the notion of an effective potential barrier in the calculation at $r \approx r_c$. The quadratic CAP

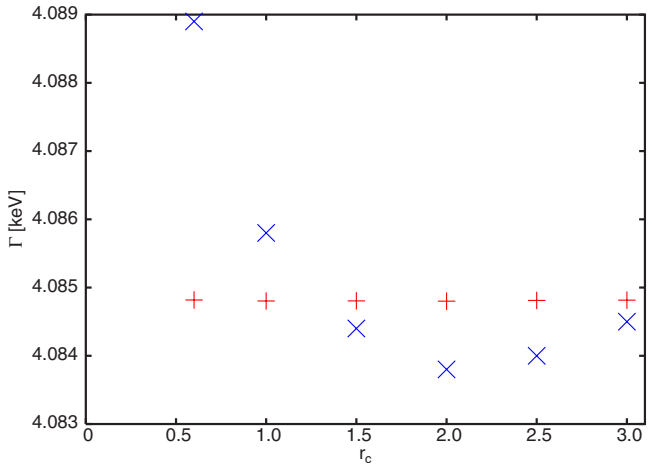

FIG. 3. (Color online) The width $\Gamma(1S\sigma)$ as a function of r_c (in units of $\hbar/mc$) for a linear (×) and a quadratic (+) CAP, as obtained in a basis specified by $N=2000$ and $s=6000$ for the U-Cf ($R=20$ fm) system.

calculation is deemed to be less sensitive to the value of r_c due to the gradual turn-on of the absorber with continuous derivative. Obviously it leads to more accurate results and will be used in the subsequent comparisons. Both CAP calculations do provide, however, consistent results for the complex resonance energy.

In Fig. 4, our results for the different analytic continuation methods are compared for the $U^{92+}+Cf^{98+}$ system at $R=20$ fm. The resonance energy $E_{\rm res}$ and the width Γ are shown as a function of the mapping parameter s [cf. Eq. (2)] for a fixed mesh size of $N=2500$ collocation points for the CS method and $N=2000$ points for the quadratic CAP method. The linear CAP results would be indistinguishable from the $n=2$ results on the scale of the figures.

We find that the CS and CAP ($n=2$) methods return consistent results within a parameter range of $500<s<8000$ with small relative fluctuations. Both $E_{\rm res}$ and Γ are determined with a relative accuracy of better than 10^{-4}. For values of the mapping parameter s outside of the ideal range the uncertainties increase, particularly so for the width.

Also shown in Fig. 4 are two results for the same system from Ref. [5]. They deviate among themselves on the same scale approximately as from the present values derived from the CS and CAP methods. Not shown are the results from the Breit-Wigner fits based on the diagonalization of the Hermitian Hamiltonian matrix in the Fourier grid method. We note, however, that $E_{\rm res}$ is predicted in close agreement with the CAP or CS data, while Γ is overestimated. For the projection method it happens to agree with the result from a phase-shift analysis performed in Ref. [5].

In order to demonstrate the convergence properties of the present CAP and CS results, we explore in Fig. 5 the dependence of Γ on the grid size N for a fixed value of the mapping parameter ($s=1000$). The data indicate a systematic variation with N for the CS data at large N, and for $N=2500$ it appears as if the width is established to four significant digits. The CAP results, on the other hand, display better convergence at $N=1000$ already, with a deviation of less than 20 meV from the $N=2000$ result. The stability of

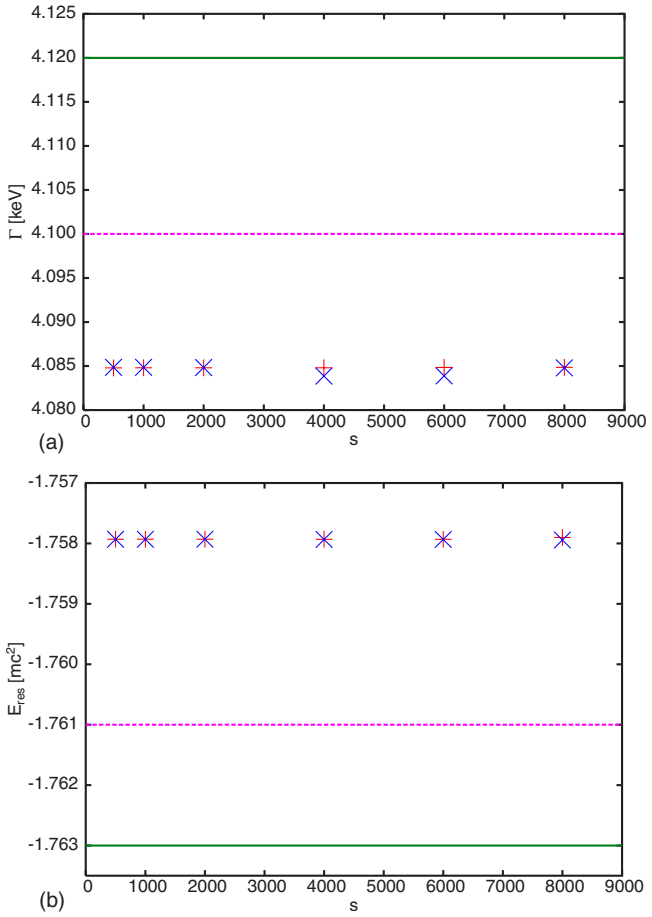

FIG. 4. (Color online) The width $\Gamma(1S\sigma)$ and mean energy $E_{\mathrm{res}}(1S\sigma)$ for the U-Cf ($R=20$ fm) system as a function of the mapping parameter s [cf. Eq. (2)] with $N=2500$ points for the CS method ($\times$) and $N=2000$ points for the CAP method (+). The lines indicate values from Ref. [5], the phase-shift result is given as a solid line, and the truncated potential method result as a dashed line.

E_{res} for different grid sizes is on the order of $10^{-8}mc^2$ for both methods and so it is stable for all N values shown.

To generalize our results from the test case of a U-Cf quasimolecule at $R=20$ fm to other situations, we have explored the relationship between the resonance position and width. In Fig. 6, Γ is shown as a function of E_{res} over a substantial range of system parameters. On the scale of the graph, differences between the present data and previous literature results cannot be noticed, i.e., they follow an almost universal curve. A number of the data points were obtained from different quasimolecular systems at various internuclear separations with both point and extended nuclear models (in monopole approximation). Data from single-center calculations with one extended nucleus also follow the same relationship.

The data displayed in Fig. 6 demonstrates that the mapped Fourier grid method provides an accurate discretization in order to represent resonances embedded deeply in the negative continuum. We find that small changes to the potential (single-center vs monopole approximation to the two-center Coulomb interaction), or changes to the method of deriving

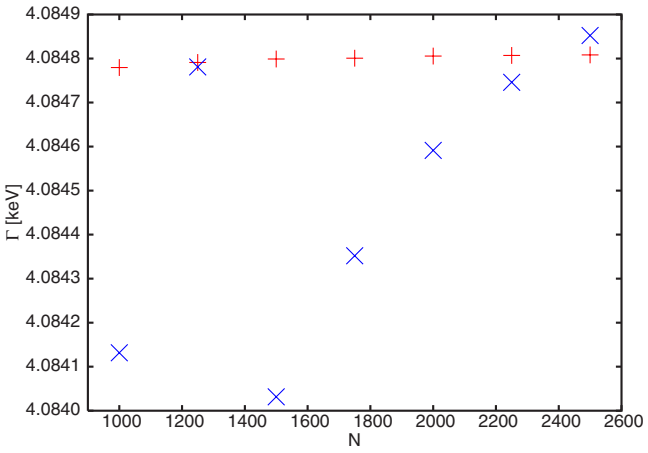

FIG. 5. (Color online) The width $\Gamma(1S\sigma)$ as a function of mesh size N using the CS ($\times$), and quadratic CAP (+) methods with mapping parameter $s=1000$ for the U-Cf ($R=20$ fm) system.

the resonance parameters, such as represented by those used in Ref. [5] or the Hermitian projection and density of states methods result in small deviations from the E_{res} vs Γ relationship displayed in Fig. 6. These deviations are on the scale of up to a percent, such as displayed in Fig. 3. We carried out calculations with the quadratic CAP method for the U-Cf system with distances in the vicinity of $R=20$ fm to explore whether one of the data pairs $(E_{\mathrm{res}},\Gamma)$ from Ref. [5] could be reproduced accurately, and found this not to be the case.

IV. CONCLUSIONS

Analytic continuation by a complex absorbing potential was applied to the Dirac equation and shown to provide a robust technique for computing supercritical resonances when using the mapped Fourier grid method to generate a

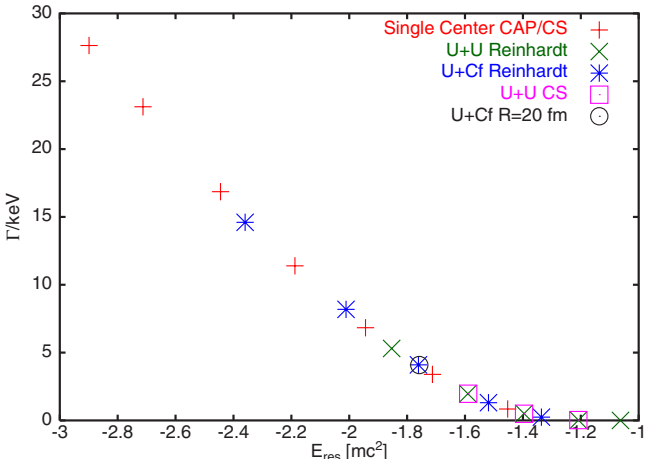

FIG. 6. (Color online) The width $\Gamma(1S\sigma)$ as a function of $E_{\mathrm{res}}(1S\sigma)$ calculated by different methods and using different supercritical potentials. The U-U and U-Cf data from Ref. [5] were obtained for the distances $R=16^{*}$, 16, 20, 25, 30 fm, while the single-center CAP/CS data from the present work were obtained for $Z=195,193,190,187,184,181,178$. The leftmost U-U and U-Cf points marked by $R=16^{*}$ fm were calculated with pointlike nuclei.

matrix representation of the Hamiltonian. Both a linear and a quadratic CAP potential were used and gave consistent results. The quadratic CAP was found to be superior due to the virtual independence of the results on the choice of the boundary parameter r_c, where the absorber kicks in.

Analytic continuation by complex scaling has also been shown to be an accurate method for computing supercritical Dirac resonance parameters. Its advantage of introducing a single parameter with a well-defined optimization criterion was found to be offset by the need of larger matrix sizes within the mapped Fourier grid method.

The mapped Fourier grid method without analytic continuation is capable of representing the spectrum to a degree where the resonance parameters can be estimated on the basis of overlap matrix elements or the density of states. Its implementation is straightforward as there is no dependence on external parameters and subsequent optimization.

Thus, it has been shown that a problem with somewhat uncertain results, which were obtained a number of years ago, can now be solved systematically to a desirable level of precision. The advantage of the analytic continuation methods is that they yield a unique result free of any fitting procedures.

Finally, we note that the mapped Fourier grid method with quadratic CAP or with CS is well-suited to investigate effects beyond the monopole approximation to the two-center supercritical potential. We also anticipate that time-dependent relativistic collision calculations based on these techniques will offer advantages over previous calculations.

ACKNOWLEDGMENTS

The authors would like to thank Igor Khavkine for useful discussions. Financial support by NSERC Canada is gratefully appreciated.

[1] W. Greiner, *Relativistic Quantum Mechanics: Wave Equations*, 3rd ed. (Springer, New York, 2000).
[2] B. Voronov, D. Gitman, and I. Tyutin, e-print quant-ph/0608221.
[3] J. Rafelski, L. Fulcher, and A. Klein, Phys. Rep., Phys. Lett. **38**, 227 (1978).
[4] B. Müller, J. Rafelski, and W. Greiner, Z. Phys. **257**, 183 (1972).
[5] J. Reinhardt, B. Müller, and W. Greiner, Phys. Rev. A **24**, 103 (1981).
[6] W. Betz, G. Soff, B. Müller, and W. Greiner, Phys. Rev. Lett. **37**, 1046 (1976).
[7] K. Rumrich, K. Momberger, G. Soff, W. Greiner, N. Grün, and W. Scheid, Phys. Rev. Lett. **66**, 2613 (1991).
[8] A. Belkacem and A. H. Sorensen, Phys. Rev. A **57**, 3646 (1998).
[9] M. Bentley, Phys. Rev. A **42**, 3826 (1990).
[10] A. T. Kruppa, P. H. Heenen, and R. J. Liotta, Phys. Rev. C **63**, 044324 (2001).
[11] I. Gilary, A. Fleischer, and N. Moiseyev, Phys. Rev. A **72**, 012117 (2005).
[12] J. Rao, W. Liu, and B. Li, Phys. Rev. A **50**, 1916 (1994).
[13] M. V. Ivanov, J. Phys. B **34**, 2447 (2001).
[14] T. N. Rescigno, M. Baertschy, W. A. Isaacs, and C. W. McCurdy, Science **286**, 2474 (1999).
[15] J. Royal and A. E. Orel, Phys. Rev. A **73**, 042706 (2006).
[16] I. A. Ivanov and Y. K. Ho, Phys. Rev. A **69**, 023407 (2004).
[17] M. Tokman, N. Eklöw, P. Glans, E. Lindroth, R. Schuch, G. Gwinner, D. Schwalm, A. Wolf, A. Hoffknecht, A. Müller *et al.*, Phys. Rev. A **66**, 012703 (2002).
[18] R. Meyer, J. Chem. Phys. **52**, 2053 (1970).
[19] E. Fattal, R. Baer, and R. Kosloff, Phys. Rev. E **53**, 1217 (1996).
[20] E. Ackad and M. Horbatsch, J. Phys. A **38**, 3157 (2005).
[21] N. Moiseyev, Phys. Rep. **302**, 211 (1998).
[22] W. P. Reinhardt, Annu. Rev. Phys. Chem. **33**, 223 (1982).
[23] U. V. Riss and H.-D. Meyer, J. Phys. B **26**, 4503 (1993).
[24] R. Santra, Phys. Rev. A **74**, 034701 (2006).
[25] H. Masui and Y. K. Ho, Phys. Rev. C **65**, 054305 (2002).
[26] S. Sahoo and Y. K. Ho, J. Phys. B **33**, 2195 (2000).
[27] R. Santra and L. S. Cederbaum, J. Chem. Phys. **117**, 5511 (2002).
[28] I. B. Müller, R. Santra, and L. S. Cederbaum, Int. J. Quantum Chem. **94**, 75 (2003).
[29] M. Ingr, H.-D. Meyer, and L. S. Cederbaum, J. Phys. B **32**, L547 (1999).
[30] R. Santra, R. W. Dunford, and L. Young, Phys. Rev. A **74**, 043403 (2006).
[31] R. Lefebvre, M. Sindelka, and N. Moiseyev, Phys. Rev. A **72**, 052704 (2005).
[32] G. Soff, W. Betz, J. Reinhardt, and J. Rafelski, Phys. Scr. **17**, 417 (1978).